Received Date : 06-Jun-2016

Revised Date : 15-Nov-2016

Accepted Date : 11-Jan-2017

Article type : Original Manuscript

Title: Lake sedimentological and ecological response to hyperthermals: Boltysh impact crater, Ukraine

Running title: Lake formation of Boltysh impact crater lake

Alena Ebinghaus*[1] and David W. Jolley[1], Steven D. Andrews[2], David B. Kemp[1]

*corresponding author

[1]University of Aberdeen, Department of Geology and Petroleum Geology, Meston Building, Aberdeen AB24 3UE, UK, email: aebinghaus@abdn.ac.uk

[2]CASP, West Building, 181A Huntingdon Road, Cambridge CB3 0DH, UK

Associate Editor – Daniel Ariztegui

ABSTRACT

The Boltysh meteorite impact crater, Ukraine, formed at the Cretaceous-Paleogene boundary at *ca* 65.2 Ma. A borehole drilled in the central part of the crater cored a >400 m thick high-resolution lacustrine succession that covers the Dan-C2 hyperthermal event associated with a negative carbon isotope excursion. Continuous terrestrial records of past hyperthermals are of limited availability, which makes this record a unique case study of the continental impact of rapid climate warming. This study uses high-resolution sedimentological core log data together with thin section, X-ray diffraction,

This is an Accepted Article that has been peer-reviewed and approved for publication in the *Sedimentology*, but has yet to undergo copy-editing and proof correction. Please cite this article as an "Accepted Article"; doi: 10.1111/sed.12360

microprobe and palynological analyses to: (i) reconstruct lake sedimentological and ecological development across the carbon isotope excursion; and (ii) assess the environmental effect of hyperthermals on terrestrial ecosystems. Based on detailed facies analysis, five gradual stages of lake formation are identified, which show a strong relationship to carbon isotope shifts and associated climatic trends. Initially, sediment supply into the Boltysh lake was controlled by crater morphology. During later lake stages, sediment supply was increasingly controlled by changes in inflow-evaporation ratios which affected seasonal stratification patterns and longer-term lake levels. An inferred increase in atmospheric pCO_2 related to the carbon isotope excursion, together with increasing mean annual temperatures, was probably responsible for periodic increases in biological activity of photosynthesising organisms and biomass production. These fluctuations in facies and lake settings largely correspond to orbital-paced moisture availability oscillations. The gradual reduction in sediment supply commencing during early lake formation prior to carbon isotope excursion inception suggest that the Dan-C2 event did not initiate sedimentary changes, but intensified sedimentary response to orbital controlled climate change.

Key words: Boltysh crater, Early Danian Dan-C2 CIE, hyperthermal, lacustrine facies, lake formation

INTRODUCTION

Hyperthermal events can be defined as geologically brief intervals of time (<<1 Ma) characterised by rapid warming and coeval changes in the environment (Zachos et al., 2008). Hyperthermals are commonly associated with pronounced negative carbon isotope excursions (CIEs), probably caused by the transfer of large amounts of ^{12}C-enriched carbon to the ocean and atmosphere system (Speijer, 2003; Cohen et al., 2007; Quillévéré et al., 2008; Westerhold et al., 2008; Bornemann et al., 2009; Zachos et al., 2008; McInerney & Wing, 2011). The majority of hyperthermal events are recorded in marine strata while terrestrial data are of limited availability, and often incomplete or poorly preserved. As a consequence, the nature and complexity of terrestrial environments and their response patterns and rates to rapid climate warming during CIEs is poorly constrained.

The Boltysh Impact Crater, Ukraine, contains an exceptionally well-preserved terrestrial Early Danian lacustrine sedimentary record. The Boltysh Crater formed through a meteorite impact before the K/Pg boundary at 65.59 ± 0.64 Ma (Gilmour et al., 2013) on the Ukrainian Shield at the northern margin of the Tethys Ocean located in a mid-latitudinal region (Fig. 1; Kelly & Gurov 2002; Jolley et al., 2010; Daly & Jolley, 2015). Scientific drilling in 2008 in its deepest part to the west of the central peak (single borehole 42/11) revealed a >400 m thick lacustrine succession unconformably overlying Proterozoic granites and gneisses (Fig. 2; Gurov et al., 2006; Jolley et al., 2010). Measurement of bulk organic $\delta^{13}C$ revealed a significant negative excursion of *ca* -3‰ at *ca* 481 m core depth, which has been interpreted as the onset of the Dan-C2 hyperthermal (Gilmour et al., 2013).

The >400 m thick, high resolution record of borehole 42/11 offers the opportunity to assess geological and ecological changes on both long and short timescales. The present study undertakes a detailed sedimentological facies analysis by using high-resolution core log data combined with thin section, microprobe and X-ray diffraction data. Based on this analysis, lake formation is reconstructed from prior to the CIE through the entire excursion and the main factors controlling the Boltysh environment during the hyperthermal are assessed. This study aims to better understand the scope, magnitude and pace of terrestrial environmental changes during past CIEs, and their interplay with climatic variations.

METHODS

Sedimentological investigations of borehole 42/11 involved detailed core logging and recording of lithology, sedimentary structures and fossil content. Standard thin sections were produced by *t-section* (Dorset, UK) and analysed using a Meiji-MT polarizing microscope (Meiji Techno, Saitama, Japan). Photomicrographs were made with an Infinity-1-5C (Lumenera Corporation, Ottawa, ON, Canada) and Zeiss AxioScan Z1 Slide Scanner (Carl Zeiss AG, Oberkochen, Germany).

A total of 13 X-ray diffraction patterns were acquired on powder samples using an X'Pert and Empyrean PANalytical diffractometer (PANalytical, Almelo, The Netherlands) in standard reflectance geometry using mixed Cu-k$\alpha_{1/2}$ radiation (X'Pert, wavelength = 1.5425 Å), and

monochromatic Cu-kα_1 radiation (Empyrean, wavelength = 1.5406 Å). Patterns were collected from 80° 2 theta with a 0.013 step size and a total collection time of 40 min (X'Pert) and 20 minutes (Empyrean). When possible, crystalline phases were identified by comparison to the International Centre for Diffraction Data Powder Diffraction Files (ICDD PDF).

Microprobe analysis was carried out with a Microscan MK5 electron microprobe (Cambridge Scientific Instruments Limited, Cambridge, UK) using Link Analysis AN10/25S system (Link Analytical, High Wycombe, UK) for energy dispersive analysis. The beam was defocused to approximately 15µm with a live time set to 100 s (see supporting material).

Palynological and bulk organic matter δ^{13} data are adopted from Gilmour et al. (2013) and Jolley et al. 2015). Total organic carbon (TOC) profile data are taken from Gilmour et al. (2014).

BOLTYSH FACIES ASSOCIATIONS

The interval 581.6 to 181.5 m of borehole 42/11 comprises a lacustrine succession of interbedded mudstones, sandstones, conglomerates, carbonates and evaporites. Based on visual description, geochemical and mineralogical investigations 17 lithofacies with distinct grain size, composition and sedimentary structures can be distinguished (Table 1). These lithofacies are grouped into eight facies associations (FAs) according to occurrence and vertical variations of lithofacies (Table 2). The facies associations relate to proximity to the lake margin and predominating sediment transport mechanisms.

Facies Association 1: Mud-rich shallow lake (FA_{MS})

Description

The mud-rich shallow lake facies association is composed of medium grey to dark grey structureless and faintly laminated organic-rich, clay-rich or calcerous mudstones, interbedded with normal graded fine-grained sandstones and silt-rich mudstones (Figs 4A and 6A). The facies commonly contains monospecific ostracods (species not specified, Fig. 9A), and plant macrofossils, including rootlets, woody material and leaves of ferns, conifers and sclerophyllous angiosperms (Fig. 9B, Daly & Jolley

2015). Typical thickness of the mudstone packages is 20 to 40 cm. The mud-rich shallow lake facies association occurs commonly together with FA_{SIS}, FA_{SAS} and FA_{D}.

Interpretation

The presence of rootlets within structureless or faintly laminated organic-rich and clay-rich mudstones reflects vegetated, quiet marginal zones (Cabrera & Saez, 1987; Reading & Collinson, 1996) and indicates early stages of soil formation (Schieber, 1999). Sedimentation occurred under mostly oxic conditions, but may have turned anoxic temporarily based on the presence of organic-rich mudstones. Traces of significant bioturbation are not present; however, the structureless appearance of the mudstone may indicate abundant bioturbation. Interbeds of fine-grained sandstones and siltstones were probably deposited during periods of increased alluvial discharge (e.g. Styan & Bustin, 1985; Cabrera & Saez, 1987).

Facies Association 2: Sand-rich shallow lake (FA_{SAS})

Description

The sand-rich shallow lake facies association consists predominantly of silt-rich mudstones and fine-grained sandstones, intercalated with clay-rich mudstones (Figs 4B and 6B). Both siltstones and sandstones show wavy to lenticular and parallel lamination. This facies association displays slumping features which typically involve several millimetres thick packages of laminae, but which may be up to a few centimetres thick: FA_{SAS} comprises ostracods, plant remains, and occasionally fish fossils (not specified, Fig. 9C). Bioturbation is abundant in places and characterised by horizontal to sub-horizontal 1 to 3 mm wide and up to 10 mm long, straight to funnel-shaped single-branched burrows filled with sand or ostracods (Fig. 9D). Individual packages of FA_{SAS} are between 0.2 m and 4.0 m thick; they typically occur together with FA_{SIS}, FA_{MS}, FA_{CT}, F_{D} and FA_{DL}.

Interpretation

The presence of wavy to lenticular lamination in this facies association indicates deposition within an environment of elevated energy. Shore line wave action and long-shore drift of reworked river

discharge material probably produced wavy interlaminated sand and mud (Sturm & Matter, 1978; Renaut & Owen, 1991; Schieber, 1999; Tänavsuu-Milkeviciene & Frederick Sarg, 2012). Grain-size range and lamination style suggest deposition above the fair weather wave base (FWWB) within a shallow lake which is subject to high sediment supply. High sediment input together with increased wave action could have caused slope failure and remobilization of unconsolidated material associated with slumping present in this facies association (Potter et al., 2005).

Facies Association 3: Silt-rich shallow lake (FA_{SIS})

Description

The silt-rich shallow lake facies association is characterised by up to 120 cm thick beds of laminated silt-rich mudstones interbedded with several decimetres thick laminated clay-rich and organic-rich mudstones (typically up to 40 cm thick), and thin layers of laminated to structureless fine-grained sandstones . This facies association may further contain packages of pebbly mudstone, thin layers of calcite crystals, laminated calcerous micrite and ostracod bioclasts. Fossil plant leaves and plant debris are abundant, while fossil fish bones tend to occur less frequently. Abundant bioturbation are similar to those in FA_{SAS}. Packages of FA_{SIS} are typically between 5 cm and 180 cm in thickness, and predominantly occur together with FA_{SAS} and FA_{DL} (Figs 4A, 5B, 5C and 6C).

Interpretation

The high proportion of laminated siltstone beds reflects relative continuous moderate sediment supply under low energy conditions in shallow to transitional deep lake setting. The presence of lamination together with the lack of cross-rippled or lenticular lamination indicates deposition from suspension settling and underflows below FWWB and storm weather wave base (SWWB, Trewin, 1986, Schieber, 1999). Occasional beds of structureless to laminated sandstones were probably transported and deposited through fine-grained turbidity currents (Sturm & Matter, 1978; Renaut & Tiercelin, 1994), which originated along the margin during increased alluvial discharge. The preservation of interbedded organic-rich mudstones suggests phases of decreased sediment supply. Beds of micrite

and ostracod bioclasts formed in settings of low siliciclastic input and indicates elevated water pH and temperatures (Kelts & Hsü, 1978).

Facies Association 4: Deep lake laminites (FA_{DL})

Description

The deep lake laminite facies association is composed of couplets and triplets of clastic (silt and/or clay) and organic matter laminae (Figs 5A and 6D). Couplets of silt to clay and organic matter are the most common laminite type, while triplets of silt, clay and organic matter are recognised less frequently. Clastic laminae are typically <0.5 mm thick and are ungraded to normal graded. Organic laminae are usually thinner with thicknesses <0.1 mm. Both type of laminae show sharp parallel to slightly wavy boundaries (Fig. 7A): FA_{DL} is occasionally interbedded with packages of pebbly mudstone and calcite layers <1 cm thick. Slumping structures are a common feature within this facies association and affect laminite packages from a few millimetres to a few centimetres thick. Horizontal burrows similar in shape and size to those in FA_{SAS} are abundant in places, whereas fish bones, plant debris and ostracods are less common. Individual packages of this facies association are between a few centimetres and 180 cm thick and occur together with FA_{SIS} and FA_{OD} (Fig. 4A).

Interpretation

The occurrence of regular couplets and triplets of organic matter and clay to silt-sized clastic sediment is interpreted as the product of seasonal sedimentation under low energy conditions. Organic matter could be either derived from organic soil or plant litter and transported into the system as detritus or dissolved matter (Zolitschka et al., 2015), or be linked to phases of algal blooms and increased bioproductivity (Rayner, 1963; Donovan, 1975; Trewin, 1986). Increased algal productivity was probably triggered by warming temperatures (Dean et al., 1999; Andrews et al., 2010) and nutrient overturns during spring time. Preservation of organic matter and their decay products commonly requires anoxic lake bottoms (Trewin, 1986; Kemp, 1996). The deposition of clay and silt laminae suggest clastic influx into the lake, which would have occurred through wind and river discharge (Trewin, 1986). This would have been distributed through suspension settling, discrete overflows and

underflows or thin turbidity flows (Sturm & Matter, 1978; Trewin, 1986; O'Brien, 1996). The presence of bioturbation in clastic laminae indicates that at this stage of deposition lake bottom waters were well mixed and oxygen-enriched (Kelts, 1988). The lamination style of FA_{DL} suggests seasonal shifts in clastic input, coupled with variations in bioproductivity and lake stratification, with alternating laminae forming on an annual to subannual scale within a perennial lake setting (Trewin, 1986; Donovan, 1980; Anderson, 1996; O'Brien, 1996; Andrews et al., 2010, Zolitschka et al., 2015).

Facies Association 5: Organic-rich deep lake (FA_{OD})

Description

The organic-rich deep lake facies association is characterised by finely laminated (<1 mm) dark grey to black organic-rich mud and medium grey siliciclastic silt and clay (Figs 4C, 7B and 7C). Small-scale slumping occurs within packages of laminae up to several millimetres thick. Small calcite nodules 1 to 5 mm in diameter are common amongst occasional layers of ostracods and precipitated crystalline calcite. Plant remains and bioturbation are rare to absent. Individual packages are up to 120 cm thick and commonly occur together with FA_{DL} and occasionally with FA_{SIS} and FA_{D}.

Interpretation

The high organic content in FA_{OD} together with low clastic deposition indicates reduced sediment supply associated with increased biomass productivity during algal blooms. Unlike FA_{DL}, the formation of laminites is less distinctive, which suggests that seasonal changes of sedimentation at this part of the succession are less pronounced. The presence of thick packages of organic-rich mud and the lack of bioturbation suggests long periods of an oxygen-depleted hypolimnion and the lack of complete water mixing (Kelts, 1988; Talbot, 1988; Tänavsuu-Milkeviciene and Frederick Sarg, 2012). The absence of wave action indicates deposition below the FWWB under quiet relative deep lake conditions (Håkanson, 1982).

Facies Association 6: Deposits from density currents

This facies association is divided into three different types of deposits from gravity-driven density currents according to grain size and distinctive sedimentary structures, including coarse-grained turbidites, fine-grained turbidites and debris-flow deposits.

Facies Association 6.1: Coarse-grained turbidites (FA_{CT})

Description

The coarse-grained turbidite facies association is dominated by beds of structureless fine to coarse-grained (pebbly) sandstones and conglomerates, which all typically grade into laminated silt or clay-rich mudstones (Figs 5B and 7D). Individual beds display sharp and occasional erosive bases. Slumping often occurs within the lower part of the bed, but may also be recorded in the upper part. The finer grained elements of this association comprise fossil plant remains. Packages of FA_{CT} are up to 120 cm thick and often occur together with FA_{D} and FA_{SAS}.

Interpretation

The sedimentary structures recognised in this facies association indicate transport and deposition by turbidity currents (Kuenen & Migliorini, 1950; Sturm & Matter, 1978; Renaut & Tiercelin, 1994; Mutti et al., 2009; Talling et al., 2012). The basal structureless sandstone and conglomerates grading into finer grained sequences suggest deposition of high density turbidites turning into low density turbidite mudstones (e.g. Talling et al., 2012). This sequence is typically overlain by laminated fine-grained to very fine-grained sandstone and laminated mudstones, which represent waning dilute flows probably under lower stage plane bed conditions (Talling et al., 2012). Texture and grain size of this facies association indicate a proximal source. The great thickness of individual packages suggest that crater flank collapse and slope failure would have caused the majority of FA_{CT} deposits. Increased river discharge probably promoted slope failure and initiation of density currents.

Facies Association 6.2: Fine-grained turbidites (FA_{FT})

Description

The fine-grained turbidite facies association comprises similar sedimentary sequences as FA_{CT}, but comprises beds of structureless fine-grained sandstones and parallel to cross-laminated silt-rich mudstones, which typically grade into laminated silt- to clay-rich mudstones (Figs 4C, 5A and 8A). It further differs from FA_{CT} by the lack of grain sizes exceeding fine-grained sandstones, and by occasional normal graded or non-graded beds of ostracod bioclasts, marlstones and carbonate micrites. Small-scale slumping and plant remains are common. Individual packages often display sharp bases with thicknesses of up to 30 cm. Beds of FA_{FT} often show vertical grading into FA_{OD}, FA_{DL} and less commonly into FA_{SAS}, which may complicate identifying clear boundaries.

Interpretation

The sedimentary structures and grading style of FA_{FT} indicates transport and deposition from turbidity currents. The presence of cross-lamination record deposition from relatively dilute and fully turbulent flows and rather low sediment fallout rates. Normal graded grain size and occasional sudden grain-size break indicate waning flow rates in the upper part of the turbidite beds (Talling et al., 2012), In contrast to FA_{CT}, FA_{FT} represent more distal deposition commonly in the deeper parts of the lake (e.g. Sturm & Matter, 1978; Tänavsuu-Milkeviciene & Frederick Sarg, 2012); they also may be associated with periods of increased river discharge and smaller-scale slope failure. Beds of ostracod bioclasts, marlstone and carbonate micrite turbidites originated in shallow lake settings characterised by reduced sediment supply, higher pH and temperature conditions (Kelts & Hsü 1978).

Facies Association 6.3: Debris flow deposits (FA_{D})

Description

This facies association is characterised by beds of structureless, typically non-graded pebbly mudstones and sandstones, with less frequent normal or reverse grading occurring towards the top (Figs 5C and 8B). Clasts embedded in mudstones are typically granule to pebble-sized and show signs of plastic deformation. Pebbly sandstone beds comprise mud clasts, which are embedded in a mud-

rich sand to clean fine to medium-grained sand matrix. Intervals of slump structures and randomly distributed fragments of charcoal and plant debris are common. Individual beds usually display sharp boundaries, with thicknesses ranging from a few centimetres to 80 cm. Deposits of FA_D may occur together with a variety of facies associations, but occur most commonly with FA_{SIS}, FA_{CT} and FA_{SAS}.

Interpretation

The structureless texture and poor sorting of this facies association is indicative of deposition from debris flows (Middleton & Hampton, 1970; Mulder & Alexander, 2001; Talling et al., 2012). The varying mud content in the matrix of FA_D suggests that debris-flow behaviour varied between cohesive and poorly-cohesive (Talling et al., 2012). This facies association is most likely to have originated from crater flank collapse and slope failure during phases of increased sediment discharge, and could have transformed into turbidites in more distal settings (e.g. Mulder & Alexander, 2001). This is supported by packages of FA_D, which are frequently overlain by FA_{TC} and FA_{FT}.

LAKE FORMATION

Borehole 42/11 reveals a continuous succession of *ca* 400 m of lacustrine sediments, with a 60° unconformity between the impact breccia and overlying sedimentary rock at 581.9 m. Based on facies associations, mineralogical composition and palynoflora recovered in borehole 42/11, 5 distinct lake phases are distinguished. A summary of the main lake stage characteristics is provided in Table 3.

Lake stage 1

Lake stage 1 comprises the lower most 90 m of the lacustrine succession and describes a clastic-dominated shallow lake of which approximately the lower most 30 m are dominated by fining-up sequences of turbidites (FA_{CT} and FA_{FT}), interbedded with debris flow deposits (FA_D) and less frequent silt-rich shallow lake deposits (FA_{SIS}). From *ca* 550 m onwards, FA_{SIS} becomes gradually more abundant, associated with a reduction in turbidite and debris-flow deposits (Fig. 10). The majority of turbidite and debris-flow sediments probably originated from early crater collapse and

alluvial re-distribution of bedrock along the crater slope. The early stage high erosion rates could have been promoted by insufficient vegetation cover adding to the level of slope instability. Proximal debris-flow and coarse-grained turbidites grade into finer-grained turbidite facies in more distal, central lake settings. A 90 cm thick light red-coloured interval starting at 580.4 m (Fig. 11) is interpreted as a short-term marine influence from the presence of marine dinocysts (Jolley et al., 2010). This marine influence could be explained by the Early Danian sea-level rise (Adatte et al. 2002), and the crater's close proximity to the Tethyan coast, which would allow marine-influenced groundwater to intermix with the lacustrine environment (see Fig. 1). The upper part of stage 1 is characterised by a gradual reduction in clastic sediment supply.

The first evidence of lacustrine benthic fauna is recorded from subhorizontal single-branched sand-filled burrows (10.8 m above the base at *ca* 571.1 m), accompanied by increasing abundant organic matter, plant debris and charcoal fragments. Occasional layers of monospecific non-diagnostic ostracods appear at 555.5 m followed by fish fossils (unspecified) and gastropod shells of *Viviparus* (Fig. 9E) from 542.5 m onwards. The abundant chlorophycean algae *Botryococcus braunii* indicate eutrophic freshwater lake conditions (Tappan, 1980; Jolley et al., 2010) which formed shortly after the impact. Jolley et al. (2013) noted cyclic shifts in the palynological assemblages expressed by low-diversity Pinaceae (pines), Cyatheaceae (tree ferns), Polypodiaceae (ferns) and Cupressaceae (cypress family) dominated plant communities changing to high-diversity Normapolles, Juglandaceae (hickory family) and Platanaceae (plane trees) dominated flora. These cyclic shifts represent alternations between warm temperate humid (mesic humid) forests and winterwet savannah-type open vegetation controlled by moisture availability. Based on the available data Jolley et al. (2013) concluded that these moisture availability oscillations (MAOs), which continue into the CIE, had an orbital origin, probably related to *ca* 21 ka precession cycles. Frequent input of charcoal fragments suggests that wildfires were an integral part of the vegetation ecosystem.

Lake stage 2

Lake stage 2 commences at *ca* 490 m and covers *ca* 60 m of core. It precedes the CIE inception by *ca* 9 m. The transition from stage 1 to stage 2 displays a gradual decrease in FA_{CT} associated with an

increasing thickness of FA_{SIS} packages and introduction of deep lake laminites (FA_{DL}) and organic-rich deep lake (FA_{OL}) facies associations, a trend which is supported by increasing total organic carbon (Fig. 12). Both deep lakes contain single laminae or lamina bundles of crystalline calcite (Fig. 8C). Precipitation of *in situ* zeolite crystals is recorded between *ca* 471 m and 445 m (Fig. 8D). This part of the succession further comprises occasional fish fossils and rootlets, accompanied by abundant ostracod-rich packages, which decrease during the CIE main phase.

The formation of clastic and organic couplets and triplets in FA_{DL} is interpreted as seasonal shifts in clastic input and biomass production, while FA_{OD} deposits are related to more prolonged phases of reduced clastic input. The sustained accumulation of organic matter suggests a high supply of nutrients (Talbot, 1988). High bioproductivity rates have been shown to withstand periods of lake water mixing without disturbing the preservation of organic matter. However, meromictic conditions tend to favour the preservation of thick beds of organic matter (Talbot, 1988) suggesting that the Boltysh lake was mostly meromictic at this stage. The presence of the shallow lake facies FA_{SIS} reflects periodic phases of low lake levels. The presence of calcite and zeolite precipitates within various facies indicates that the lake water was periodically saline alkaline (Chipera & Apps, 2001; Langella et al., 2001; Warren, 2006), an interpretation supported by the absence of the freshwater algae *B. braunii* from this part of the succession (Jolley et al., 2015).

Palynological data record a gradual increase in abundant savannah-type open canopy flora dominated by Normapolles and juglandaceaen pollen associated with a decline in mesic humid taxa. This indicates higher mean annual temperatures and reduced moisture availability within a dry winterwet climate (Jolley et al., 2010; Daly & Jolley, 2015; Jolley et al., 2015). This trend implies a decrease in mean annual precipitation and possibly a shift towards ephemeral drainage. The presence of juglandaceous palynomorphs indicates the spread of intra-crater wetland environments possibly linked to phases of lower lake levels (Gilmour et al., 2013; 2014).

Lake stage 3

Lake stage 3 commences at *ca* 430 m core depth and covers the interval between the CIE mid-stage and the onset of the recovery stage (60 m in total). This interval is characterised by a continued

occurrence of FA_{DL} and FA_{OD} interbedded with FA_{SIS}. The savannah-type palynoflora continues to represent the dominant vegetation at this stage (Jolley et al., 2015). Unlike stage 2, stage 3 shows an influx of FA_{SAS} suggesting phases of increased shore current activity and/or wave energy. Occasional mud rip-up clasts within FA_{FT} could be sourced from subaerial exposure of lake margins or ephemeral stream beds during dry phases. The presence of synaeresis cracks is likely to be caused by compaction or salinity changes (Plummer & Gostin, 1981).

Lake stage 4

Lake stage 4 starts at *ca* 370 m and covers the onset of the positive excursion and recovery phase following the CIE main body (*ca* 65 m in total). This interval is characterised by increasingly prolonged phases of high sediment supply under elevated energy conditions (FA_{SAS}), interbedded with lower sediment supply deposition under reduced energy conditions (FA_{SIS} and FA_{MS}) in an overall shallow lake setting. The prolonged phases of elevated energy and deposition of FA_{SAS} might refer to a wind-driven lake type described in Nutz et al. (2016). The prolonged and continuous deposition of silt-rich lithofacies associated with influx of sand-rich beds in the upper part suggests relative stable aggradational sedimentation. Abundant *Milfordia hungarica* (a Restionaceae aquatic marginal monocot), *Viviparus* and *Glycimeris* communities (Fig. 9F; Gilmour et al., 2014; 2013) and varying amounts of zeolite phases suggest brackish to saline alkaline water conditions. Macrofossils and bioturbation decline rapidly at the end of stage 4 (*ca* 304 m core depth), and partially recover during the following stage.

Lake stage 5

Lake stage 5 comprises the late stage of CIE recovery and post-excursion time. The increasing thickness of FA_{SIS} packages recognised in stage 4 continues into the post-excursion interval indicating continuous prolonged deposition in a shallow lake setting. Abundant slickensides and rip-up mud clasts suggest initial soil forming processes within marginal settings associated with subaerial exposure or ephemeral drainage. The occasional occurrence of FA_{CT} beds suggests phases of

increased sediment discharge into the lake. Similar to stage 4, stage 5 is characterised by mostly aggradational deposition.

From the early recovery stage, the borehole displays an increase in abundant Cupressaceae and Pinaceae pollen, associated with an increase in fagaceous and myricaceous (sweet fern) pollen during late recovery and post-excursion stage. This reflects a return to temperate climates. This cooling trend is coincident with a shift from brackish to freshwater water implied by the abundant freshwater green algae *Pediastrum bifidites* (Gilmour et al., 2014; 2013).

DISCUSSION

Sedimentological–hydrological development

The presence of evaporative sediments and regular lake level fluctuations suggest an overall underfilled (e.g. Carroll & Bohacs 1999; Bohacs et al. 2000), closed lake setting. Initial lake formation (stage 1) is characterised by high clastic sediment input probably caused by a combination of crater slope failure and surface water runoff (Fig. 13). From the middle of stage 1 onwards (at *ca* 525 m core depth), a gradual reduction in sediment supply is inferred. With the onset of stage 2, the succession comprises deep lake facies interbedded with shallow lake facies associations and evaporative sediments. At this stage, palynological data record a gradual transition to savannah-type palynoflora associated with increasing mean annual temperatures and reduced moisture availabilities. Despite substantial lake level fluctuations and evaporative phases, there is no obvious evidence of subaerial exposure and complete desiccation, which suggest that sufficient water supply was maintained through the drier periods. A possible explanation for maintaining a perennial lake setting could be seasonal high precipitation and surface water runoff, and relatively continuous groundwater inflow.

The formation of regular lamina couplets and triplets in the deep lake facies associations indicates regular variations in clastic input and bioproductivity. This type of lamination is interpreted to have formed in a stratified biologically active lake which was subject to regular lake turn-overs. The formation of a stratified lake could be related to a more intense seasonal climate resulting in periodic

lake turn-overs accompanied by algal blooms. The lake water becoming periodically more saline alkaline might have promoted meromictic conditions by forming a chemocline and separating water masses of different salinity levels (Löffler, 2004).

The CIE mid-stage (lake stage 3) is characterised by increasingly prolonged intervals of shallow lake facies associations. Occasional deposition of rip-up clasts and formation of synaeresis cracks suggest periods of further reduced lake levels and variable water chemistry, supported by palynoflora adapted to an increasingly dry and warm climate. Intermittent deposition of FA_{SAS} could be the result of re-transported sediment along the shoreline during phases of high wave activity and high sediment supply.

Lake stage 4 marks the beginning of the positive excursion and is particularly characterised by a distinctive decline in FA_{DL} and FA_{OD}. Palynological investigations indicate a gradual return to wetter and cooler climates. This trend is reflected by a transition from saline to brackish conditions, a gradual increase in clastic sediment input and reduction in lake stratification features. The increase of bioturbation may be related to regular mixing of oxygen- and nutritious-rich waters with less productive lake zones.

The transition from lake stage 4 to stage 5 is marked by a rapid decline in abundant macro fauna at the end of the CIE recovery time. With the end of the recovery phase, TOC declines (Fig. 12). Similar to lake stage 4, stage 5 is characterised by thick packages of FA_{SIS} and FA_{SAS}, demonstrating stable depositional conditions and lake levels. The return to freshwater conditions was accompanied by better water mixing. This is supported by a decrease in TOC to levels similar to those at pre-CIE time, suggesting an oxygenated and well-mixed lake bottom conditions. Seepage and groundwater inflow was possibly reduced due to the deposition of a less permeable clay-rich layer during lake stages 2 and 3. Frequent sand-rich intervals and occasional proximal turbidite sequences indicate regular sediment supply. At this stage sediment was probably mostly supplied by surface water runoff which corresponds to the increasingly wetter climate (Fig. 13).

Environmental factors

The sedimentary record of borehole 42/11 and the timing of the Dan-C2 CIE suggests a link between reduction in clastic sediment supply and the Early Danian carbon isotope profile. During the pre-CIE interval, sediment input was controlled by both crater morphology and the unconsolidated ejecta blanket. Based on models by McGetchin et al. (1973) and Collins et al. (2005), the height of the ejecta blanket varied between 120 m and 350 m. Initially high erosion rates of the crater slope and the ejecta layer would have provided the high amount of sediment deposited into the lake. This was probably promoted by open canopy vegetation during dry phases providing less soil stability than closed canopy forests during wetter phases (Jolley et al., 2015). Gradual slope stabilization and shallowing led to a decrease in clastic sediment supply. During the CIE main phase (lake stages 2 and 3) sediment was deposited periodically probably due to seasonal changes in mean annual precipitation and drainage of the crater rim. This would have caused the fluctuations of shallow and deep lake facies associations which are recognised in this part of the succession. The return to cooler and wetter climatic conditions in the recovery and post-excursion interval associated with prolonged phases of clastic deposition suggest that at this stage slope drainage and clastic sediment supply increased and was more constant. In comparison, sedimentological and climatic investigations of the Pliocene El'gygytgyn crater lake, north east Siberia (Asikainen et al., 2007), and the Late Pleistocene-Early Holocene Bosumtwi crater lake, Ghana (Shanahan et al., 2006; Brigham-Grette et al., 2007), do not record initial high erosion rates of the crater, but suggest a strong climatic control on lake level changes and sediment input.

Increased TOC values during the main and recovery phase of the CIE and increased deposition of organic matter during lake stages 2 and 3 suggest a causal link between the Dan-C2 CIE trend and the occurrence of organic-rich facies. Production of organic matter is generally controlled by availability of CO_2, O_2, and nutrients, with CO_2 and O_2 influencing photosynthesis, respiration, as well as decay and preservation processes of dead organic matter at the lake bottom (Hutchinson, 1957). The proportion of CO_2 in lake water is dependent on atmospheric pCO_2 and input of dissolved carbon via surface runoff, precipitation and groundwater (Hutchinson, 1957; Wetzel, 2001; Stumm, 2004). The addition of ^{12}C enriched carbon to the atmosphere and ocean systems during the negative CIE could

have increased *p*CO2 and carbon uptake in the lake. The increased availability of carbon together with warm climatic conditions and regular mixing of the lake water during lake turn overs would have promoted bioproductivity and accumulation of organic matter. The major sink of carbon released to the atmosphere are the oceans; and at major negative CIEs, ocean acidification has occurred concomitantly with C release (Caldeira & Wickett, 2003; Zachos et al., 2008). Lakes would act as secondary sinks for excess atmospheric carbon, but the precipitation of calcium carbonate and zeolite phases in the Boltysh lake during the CIE does not support a long-term decrease in lake water pH (e.g. Hutchinson, 1957; Chipera & Apps, 2001).

Facies changes during the Dan-C2 hyperthermal

The onset of sediment supply reduction associated with a gradual shift from coarser-grained facies to clay-rich and organic-rich facies is recognised at a core depth of *ca* 528 m – predating the CIE inception by *ca* 47 m (Fig. 10). This early shift in sedimentary facies suggests gradual environmental changes relative to the Dan-C2 CIE. Studies of the Early Danian carbon isotope profile indicate orbital controls on the carbon cycle and bioproductivity (Quillévéré et al., 2008). This is supported by Jolley et al. (2015) and Jolley et al. (in prep.) who identified precession-paced moisture availability oscillations, which occurred prior to and during the CIE. Oscillations in Earth's orbital parameters control the amount and distribution of incident solar radiation (Hays et al., 1976; Zachos et al., 2001), and affect ocean and atmosphere circulation, precipitation, intensity of seasonality, global carbon cycle and pCO_2 (Ruddiman & McIntyre, 1981; Crowley et al., 1992; Herbert 1997). The moisture availability cycles recognised in the palynological record also correspond with sub-CIE scale carbon isotope cycles previously recognised by Gilmour et al. (2013) and are expressed in the deep lake facies associations between 587 m and 369 m. These deep lake facies alternate with shallow lake facies associations indicating fluctuations in lake level and sediment supply. This relationship suggests a strong sedimentological and ecological response to climatic changes associated with the Dan-C2 CIE. The presence of such pronounced and relative short-term lake level fluctuations during the hyperthermal further support the idea that seasonality became more intense during the hyperthermal. This is an environmental trend that is also recognised from Palaeocene–Eocene thermal

maximum (PETM) sites in the mid-latitude Northern Hemisphere, which record an increase in the seasonality of precipitation and storm events (McInerney & Wing, 2011).

CONCLUSIONS

Detailed analysis of borehole 42/11 sedimentology demonstrates a clear sedimentological response to the Early Danian carbon isotope excursions (CIE) and associated climate changes. Initial clastic sediment supply was mostly controlled by crater morphology, which in later lake stages became increasingly controlled by seasonal variations in inflow and evaporation linked to climate. The potential areal extent of drainage catchment area includes the crater rim and inner crater slope; however, more detailed modelling of potential crater rim uplift is required to better constrain the development of drainage catchment size.

The Dan-C2 CIE together with increasing mean annual temperatures were likely to have promoted photosynthesis and biomass production. Increased seasonality and amplified environmental changes during the hyperthermal caused more pronounced lake stratification and lake turn-overs, which is reflected in the occurrence of regular seasonal couplets in the deep lake laminite facies association. These seasonal changes were part of longer term lake level fluctuations which corresponded to orbital-paced moisture availability oscillations recognised in the palynological record.

Gradual facies changes commencing prior to and across the CIE inception indicate that initial sedimentological changes were not linked to the Dan-C2 hyperthermal. The correlation between orbitally-paced moisture availability oscillations and lake facies fluctuations implies that the CIE promoted lake sedimentological and ecological response to climate changes.

ACKNOWLEDGMENTS

Initial drilling of the Boltysh meteorite crater was funded by Natural Environment Research Council (NERC) grant NE/D005043/1. The authors are extremely grateful to the valuable scientific contributions of Simon Kelley and Iain Gilmour. The constructive and critical reviews by Mathieu Schuster and an anonymous reviewer greatly helped to improve this manuscript.

REFERENCES

Adatte, T., Keller, G. and **Stinnesbeck, W.** (2002) Late Cretaceous to early Paleocene climate and sea-level fluctuations: the Tunesian record. *Palaeogeogr. Palaeoclimatol. Palaeoecol.*, **178**, 165–196.

Anderson, R.Y. (1996) Seasonal sedimentation: a framework for reconstructing climatic and environmental change. *Geol. Soc. London, Spec. Publ.*, **116**, 1–15.

Andrews, S.D., Trewin, N.H., Hartley, A.J. and **Weedon, G.P.** (2010) Solar variance recorded in lacustrine deposits from the Devonian and Proterozoic of Scotland. *J. Geol. Soc. London*., **167**, 847-856.

Asikainen, C.A., Francus, P. and **Brigham-Grette (2007)** Sedimentology, clay mineralogy and grain size as indicators of 65 ka of climate change from El'gygytgyn Crater Lake, Northeastern Siberia. *J Paleolimnol*, **37**, 105-122.

Bohacs, K.M., Carroll, A.R., Neal, J.E. and **Mankiewicz, P.J.** (2000) Lake-Basin Type, Source Potential, and Hydrocarbon Character: An Integrated Sequence-Stratigraphic-Geochemical Framework. In: *Lake Basins Through Space and Time* (Eds. E.H. Gierlowski-Kordesch and K. Kelts),. AAPG Studies in Geology 46, 3-34.

Bornemann, A., Schulte, P., Sprong, J., Steurbaut, E., Youssef, M. and **Speijer, R.P.** (2009) Latest Danian carbon isotope anomaly and associated environmental change in the southern Tethys (Nile Basin, Egypt). *J. Geol. Soc. London*, **166**, 1135–1142.

Bouma, A.H. (1962) Sedimentology of some Flysch deposits. Elsevier, Amsterdam, 168 pp.

Bradley, W.H. (1970) Green River Oil Shale - Concept of Origin Extended An Interdisciplinary Problem Being Attacked from Both Ends. *Geol. Soc. Am. Bull*., **81**, 985–1000.

Brigham-Grette, J., Melles, M., and **Minyk, P. (2007)** Overview and significance of a 250 ka paleoclimate record form El'gygytgyn Crater Lake, NE Russia. *J Paleolimnol*, **37**, 1-16.

Cabrera, L. and **Saez, A.** (1987) Coal deposition in carbonate-rich shallow lacustrine systems: the Calaf and Mequinenza sequences (Oligocene, eastern Ebro Basin, NE Spain). *J. Geol. Soc. London*, **144**, 451–461.

Caldeira, K. and **Wickett, M.E.** (2003) Anthropogenic carbon and ocean pH. *Nature*, **425**, 365.

Carroll, A.R. and **Bohacs, K.M. (**1999) Stratigraphic classification of ancient lakes: Balancing tectonic and climatic controls. *Geology*, **27**, 99–102.

C**hipera, S.J.** and **Apps, J.A. (**2001) Geochemical Stability of Natural Zeolites. In: *Natural Zeolites: Occurrence, Properties, Applications* (Eds. D.L. Bish and D.W. Ming),. Mineralogical Society of America and Geochemical Society Reviews in Mineralogy & Geochemistry 45, 117-162.

Cohen, A.S., Coe, A.L. and **Kemp, D.B. (**2007) The Late Palaeocene-Early Eocene and Toarcian (Early Jurassic) carbon isotope excursions: a comparison of their time scales, associated environmental changes, causes and consequences. *J. Geol. Soc. London*, **164**, 1093–1108.

Collinson, J.D., Mountney, N. and **Thompson, D.** (2006) Sedimentary Structures. Terra Publishing, Harpenden, 292 pp.

Crowley, T.J., Kim, K.-Y., Mengel, J.G. and **Short, D.A.** (1992) Modelling 100,000-Year Climate Fluctuations in Pre-Pleistocene Time Series. *Science*, **255**, 705-707.

Daly, R.J. and **Jolley, D.W.** (2015) What was the nature and role of Normapolles angiosperms? A case study from the earliest Cenozoic of Eastern Europe. *Palaeogeogr. Palaeoclimatol. Palaeoecol.*, **418**, 141–149.

Dean, J.M., Kemp, A.E.S., Bull, D., Pike, J., Patterson, G. and **Zolitschka, B.** (1999) Taking varves to bits: Scanning electron microscopy in the study of laminated sediments and varves. *J. Paleolimnol.*, **22**, 121-136.

Demaison, G.J. and **Moore, G.T.** (1980) Anoxic environments and oil source bed genesis. *Org. Geochem.*, **2**, 9–31.

Donovan, R.N. (1980) Lacustrine cycles, fish ecology and stratigraphic zonation in the Middle Devonian of Caithness. *Scottish J. Geol.*, **16**, 35–72.

Donovan, R.N. (1975) Devonian lacustrine limestone at the margin of the Orcadian Basin, Scotland. *J. Geol. Soc. London*, **131**, 489–519.

Gilmour, I., Gilmour, M., Jolley, D., Kelley, S., Kemp, D., Daly, R. and **Watson, J.** (2013) A high-resolution nonmarine record of an early Danian hyperthermal event, Boltysh crater, Ukraine. *Geology*, **41**, 783–786.

Gilmour, I., Jolley, D., Kemp, D., Kelley, S., Gilmour, M., Daly, R. and **Widdowson, M.** (2014) The early Danian hyperthermal event at Boltysh (Ukraine); relation to Cretaceous-Paleogene boundary events. *Spec. Pap. - Geol. Soc. Am.*, **505**, 133–146.

Gurov, E.P., Kelley, S.P., Koeberl, C. and **Dykan, N.I. (2006)** Sediments and Impact Rocks filling the Boltysh Impact Crater. In: *Biological Processes associated with Impact Events* (Eds. C. Cockell, C. Koeberl, and I. Gilmour), Springer, 335-358.

Håkanson, L. (1982) Bottom dynamics in lakes. *Hydrobiologica*, **91**, 9-22.

Hays, J.D., Imbrie, J. and **Shackleton, N.J.** (1976) Variations in the Earth's Orbit: Pacemaker of the Ice Ages. *Science*, 194, 1121-1132.

Herbert, T.D. (1997) A long marine history of carbon cycle modulation by orbital-climatic changes. *Proc. Natl. Acad. Sci.*, **94**, 8362-8369.

Hutchinson, G.E. (1957) A Treatise on Limnology. Volume I - Geography, Physics, and Chemistry. John Wiley & Sons, 1015 pp.

Jolley, D., Gilmour, I., Gurov, E., Kelley, S. and **Watson, J.** (2010) Two large meteorite impacts at the Cretaceous-Paleogene boundary. *Geology*, **38**, 835–838.

Jolley, D.W., Gilmour, I., Gilmour, M., Kemp, D.B. and **Kelley, S.P.** (2015) Long-term resilience decline in plant ecosystems across the Danian Dan-C2 hyperthermal event, Boltysh crater, Ukraine. *J. Geol. Soc. London*, **172**, 491-498.

Kelly, S.P. and **Gurov, E.** (2002) Boltysh, another end-Cretaceous impact. *Meteorites & Planetary Science*, **37**, 1031-1043.

Kelts, K. (1988) Environment of deposition of lacustrine petroleum source rock: An introduction. In: *Lacustrine Petroleum Source Rocks* (Eds. A.J. Fleet, K. Kelts and M.R. Talbot), p. 3-26. Geological Society, London, Special Publications 40.

Kelts, K. and **Hsü, K.J.** (1978) Freshwater Carbonate Sedimentation. In: *Lakes-Chemistry, Geology, Physics* (Ed. A. Lerman), p. 295-323. Springer Publishing, New York.

Kemp, A.E.S. (1996) Laminated sediments as palaeo-indicators. In: *Palaeoclimatology and Palaeoceanography from Laminated Sediments* (Ed. A.E.S Kemp), p. vii–xii, Geol. Soc. London, Spec. Publ. 116.

Kuenen, H. and **Migliorini, C.I.** (1950) Turbidity Currents as a Cause of Graded Bedding. *J. Geol*., **58**, 91–127.

Langella, A., Cappelletti, P. and **De'Gennaro, M.** (2001) Zeolites in Closed Hydrologic Systems. In: *Natural Zeolites: Occurrence, Properties, Applications* (Eds D.L. Bish and D.W. Ming), pp. 235–260, Mineralogical Society of America and Geochemical Society Reviews in Mineralogy & Geochemistry 45.

Löffler, H. (2004) The Origin of Lakes. In: *The Lakes Handbook. Limnology and Limnetic Ecology. Volume 1* (Eds. P.E. O'Sullivan and C.S. Reynolds), pp. 8–60. Blackwell Publishing.

McInerney, F. A. and **Wing, S.L.** (2011) The Paleocene-Eocene Thermal Maximum: A Perturbation of Carbon Cycle, Climate, and Biosphere with Implications for the Future. *Annu. Rev. Earth Planet. Sci.*, **39**, 489–516.

Middleton, G.V. and **Hampton, M.A.** (1970) Sediment Gravity Flows I: Mechanics of Flow and Deposition. In: *Turbidites and Deep-Water Sedimentation* (Eds. G.V. Middleton and A.H. Bouma, A.H.), pp. 1–38. SEPM, Pacific Section, Short Course Lecture Notes.

Mulder, T. and **Alexander, J.** (2001) The physical character of subaqueous sedimentary density flow and their deposits. *Sedimentology*, **48**, 269–299.

Mutti, E., Bernoulli, D., Lucchi, F.R. and **Tinterri, R.** (2009) Turbidites and turbidity currents from alpine "flysch" to the exploration of continental margins. *Sedimentology*, **56**, 267–318.

O'Brien, N.R. (1996) Shale lamination and sedimentary processes. *Geol. Soc. London, Spec. Publ*., **116**, 23–36.

Plummer, P.S. and **Gostin, V.A.** (1981) Shrinkage cracks: Desiccation or synaeresis? *J. Sed. Petrol.*, **51**, 1147-1156.

Potter, P.E., Maynard, J.B. and Depetris, P.J. (2005) Mud and Mudstones. Introduction and Overview. Springer, Berlin, Heidelberg, New York, 305 pp.

Quillévéré, F., Norris, R.D., Kroon, D. and **Wilson, P.A.** (2008) Transient ocean warming and shifts in carbon reservoirs during the early Danian. *Earth Planet. Sci. Lett.*, **265**, 600–615.

Rayner, D.H. (1963) The Achanarras Limestone of the Middle Old Red Sandstone, Caithness, Scotland. *Proc. Yorksh. Geol. Soc.*, **34**, 117–138.

Reading, H.G. and **Collinson, J.D.** (1996) Clastic Coasts. In: *Sedimentary Environments: Processes, Facies and Stratigraphy* (Ed. H.G. Reading), pp. 154–231. Blackwell Publishing.

Renaut, R.W. and **Owen, R.B. (**1991) Shore-zone sedimentation and facies in a closed rift lake: The Holocene beach deposits of Lake Bogoria, Kenya. In: *Lacustrine Facies Analysis* (Eds. P. Anadon, L.I. Cabrera and K. Kelts, K.), pp. 175–195. International Association Sedimentologist Special Publication13.

Renaut, R.W. and **Tiercelin, J.-J.** (1994) Lake Bogoria, Kenya Rift Valley - a sedimentological overview. In: *Sedimentology and Geochemistry of Modern and Ancient Saline Lakes* (Eds. R.W. Renaut and W.M. Last), pp. 101–124. SEPM Special Publication 50.

Ruddiman, W.F. and **McIntyre, A.** (1981) Oceanic Mechanisms for Amplification of the 23,000-Year Ice-Volume Cycle. *Science*, **212**, 617-627.

Schieber, J. (1999) Distribution and deposition of mudstone facies in the Upper Devonian Sonyea Group of New York. *J. Sediment. Res*., **69**, 909–925.

Scotese, C.R. (2014) Atlas of Late Cretaceous Maps. PALEOMAP Atlas for ArcGIS, volume 2, The Cretaceous, Maps 16-22, Mollweide Projection, Evanston, IL.

Shanahan, T.M., Overpeck, J.T., Winston Wheeler, C, Warren Beck, J., Pigati, J.S., Talbot, M.R., Scholz, C.A., Peck, J. and **King, J.W. (2006)** Paleoclimatic variations in West Africa from a record of late Pleistocene and Holocene lake level stands of Lake Bosumtwi, Ghana. *Palaeogeogr. Palaeoclimatol. Palaeoecol.*, **242**, 287-302.

Speijer, R.P. (2003) Danian-Selandian sea-level change and biotic excursion on the southern Tethyan margin (Egypt). In: *Causes and Consequences of Globally Warm Climates in the Early Paleogene* (Eds. S.L. Wing, P.D. Gingerich, B. Schmitz, B. and E. Thomas, E.), pp. 275–290. Geological Society of America Special Paper 369.

Stumm, W. (2004) Chemical Processes Regulating the Composition of Lake Waters. In: *The Lakes Handbook. Limnology and Limnetic Ecology. Volume 1* (Eds. P.E. O'Sullivan and C.S. Reynolds), pp. 79–106. Blackwell Publishing.

Sturm, M. and **Matter, A.** (1978) Turbidites and Varves in Lake Brienz (Switzerland): Deposition of Clastic Detritus by Density Currents. In: *Modern and Ancient Lake Sediments* (Eds. A. Matter,

A. and M.W. Tucker), pp. 147–168. International Association of Sedimentologists Special Publication 2.

Styan, W.B. and **Bustin, R.M.** (1985) Sedimentology of Fraser River Delta Peat Deposits: A Modern Analogue for Some Deltaic Coals. In: *Sedimentology of Coal and Coal-Bearing Sequences*. (Eds A. Rahmani and R.M. Flores), pp. 241-271. IAS Spec. Publ. 7.

Talbot, M.R. (1988) The origins of lacustrine oil source rocks: evidence from the lakes of tropical Africa. *Geol. Soc. London, Spec. Publ.*, **40**, 29–43.

Talling, P.J., Masson, D.G., Sumner, E.J. and **Malgesini, G.** (2012) Subaqueous sediment density flows: Depositional processes and deposit types. *Sedimentology*, **59**, 1937–2003.

Tänavsuu-Milkeviciene, K. and **Frederick Sarg, J.** (2012) Evolution of an organic-rich lake basin - stratigraphy, climate and tectonics: Piceance creek basin, Eocene Green River Formation. *Sedimentology*, **59**, 1735–1768.

Tappan, H. (1980) The paleobiology of plant protists. W.H. Freeman, 1028 pp.

Trewin, N.H. (1986) Palaeoecology and sedimentology of the Achanarras fish bed of the Middle Old Red Sandstone, Scotland. *Trans. R. Soc. Edinb. Earth Sci.*, **77**, 21–46.

Warren, J.K. (2006) Evaporites: Sediments, Resources and Hydrocarbons. Springer-Verlag, Berlin Heidelberg, 1036 pp.

Westerhold, T., Röhl, U., Raffi, I., Fornaciari, E., Monechi, S., Reale, V., Bowles, J. and **Evans, H.F.** (2008) Astronomical calibration of the Paleocene time. *Palaeogeogr. Palaeoclimatol. Palaeoecol.*, **257**, 377–403.

Wetzel, R.G. (2001) Limnology. Lake and River Ecosystems, 3rd ed. Academic Press, 1006 pp.

Zachos, J., Pagani, M., Sloan, L., Thomas, E. and **Billups, K.** (2001) Trends, rhythms, and aberrations in global climate 65 Ma to present. *Science*, **292**, 686–93.

Zachos, J.C., Dickens, G.R. and **Zeebe, R.E.** (2008) An early Cenozoic perspective on greenhouse warming and carbon-cycle dynamics. *Nature*, **451**, 279–283.

Zolitschka, B., Francus, P., Ojala, A.E.K. and **Schimmelmann, A.** (2015) Varves in lake sediments - a review. *Quaternary Science Reviews*, **117**, 1-41.

Fig. 1: Early Palaeogene palaeogeographical map of Europe, with the location of the Boltysh impact crater near the northern margin of the Tethys Ocean indicated by the red dot (modified from Scotese, 2014).

Fig. 2: Google earth obliquity view onto the modern Boltysh impact site, Ukraine, and simplified cross-section of the sedimentary crater fill along line a–a'. Cross-section includes the location of borehole 42/11, with bolt line indicating section of core logged in this study. Dashed white circle indicates approximate extent of the crater. Cross-section modified from Jolley et al. (2013).

Fig. 3: Key to sedimentary fill patterns and symbols used in sedimentary logs in Figs 4, 5 and 10.

Fig. 4: Typical sections of facies associations logged in borehole 42/11: (A) succession of FA_{MS} – (= mud-rich shallow lake facies association) and FA_{SIS} – (= silt-rich shallow lake facies association), interbedded with FA_{SAS} (= sand-rich shallow lake facies association) between 332.8 m and 330.8 m core depth; (B) packages of predominantly wavy laminated FA_{SAS} between 383.6 m and 381.6 m core depth; (C) succession of FA_{OD} (= organic-rich deep lake facies association), interbedded with FA_{DL} (= deep lake laminite facies association) and FA_{FT} (= fine-grained turbidite facies association) between 462.1 m and 460.1 m core depth. Close-up views illustrated in Figs 6 to 8. For key see Fig. 3.

Fig. 5: Typical sections of facies associations logged in borehole 42/11 (continued from Fig. 4): (A) FA_{FT} beds interbedded with packages of FA_{DL} between 464.0 m and 462.2 m core depth; (B) packages of FA_{SIS} interbedded with FA_{CT} (= coarse-grained turbidites) between 532.0 m and 534.0 m core depth; (C) succession of FA_{D} (= debris-flow deposits), interbedded with FA_{CT} and FA_{SIS} from 538.1 to 536.1 m core depth. Close-up views illustrated in Figs 6 to 8. For key see Fig. 3.

Fig. 6: Close-up views of facies associations described in Figs 4 and 5: (A) gradual transition from laminated FA_{SIS} into structureless, organic-rich and rootlet bearing FA_{MS} at *ca* 331.4 m; (B) typical

wavy lamination of FA_{SAS} at 382.1 m, (C) laminae of siltstone and fine-grained sandstone of FA_{SIS} at 531.3 m, (D) planar laminae of clay-rich and silt-rich mudstone of FA_{DL} at 463.4 m.

Fig. 7: Close-up views of facies associations described in Figs 4 and 5: (A) thin section of FA_{DL} taken at magnitude x 5 at 483.78 m, showing laminae of organic matter, clay and silt; (B) typical succession of fissile, organic-rich laminae of FA_{OD} at 460.4 m; (C) close-up of FA_{OD} taken at magnitude x 5 at 479.72 m, showing laminae of organic matter, clay and/or silt with abundant small calcite nodules and occasional quartz grains; (D) normal graded sequence of FA_{CT} displaying the T_A and T_B divisions of a typical Bouma sequence (after Bouma, 1962). All thin section photographs taken under plane polarized light.

Fig. 8: Close-up views of facies associations described in Figs 4 and 5: (A) normal graded fine-grained turbidite (FA_{FT}) bed displaying the T_B division of a typical Bouma sequence (after Bouma, 1962) at 460.8 m. Note the calcite layer overlying the turbidite; (B) structureless, granule-rich coarse sandstone of FA_D at 537 m; (C) close-up view of calcite evaporite layer as shown in Fig. 8A; (D) individual zeolite crystals of the Heulandite–Clinoptilolite group embedded within organic-rich mudstone (FA_{OD}) at 463.4 m. All thin section photographs taken under plane polarized light.

Fig. 9: Most common macrofossils of borehole 42/11: (A) monospecific (non-diagnostic) ostracod shells at 365.5 m; (B) example of fern leaves and plant debris at 444.9 m; (C)fish fossils (not specified) at 466.1 m; (D) horizontal, ostracod-filled burrow at 400.4 m; (E) gastropod shells of *Viviparus* at 325.2 m, indicating saline to brackish lake conditions; (F) – bivalve shells of *Glycimeris* at 314.6 m, indicating mixed saline lake conditions.

Fig. 10: Borehole 42/11 sedimentary log and corresponding sediment supply, inferred water salinity and lake level changes based on facies associations. Black squares mark the positions of core sections referred to in Figs 4 and 5. Fluctuations in lake facies and lake level correlate with subordinate $\delta^{13}C$ cycles during the negative excursion ($\delta^{13}C$ data from Gilmour et al., 2013) and orbital-paced moisture

availability oscillations (= MAOs, marked by numbers 1 to 11) inferred from compositional shifts in the pollen and spore record (see Jolley et al., 2013; 2015). This is presented by the detrended correspondence analysis (DCA) axis trend, which shows cyclic shifts in the ratios of humid warm temperate vegetation to winterwet savannah-type vegetation. The correlation of MAOs with deep lake phases (purple and blue coloured units) suggests a strong climatic control on lake sedimentology and an increased environmental response during the hyperthermal. This is supported by total organic carbon data presented in Fig. 12. See Fig. 3 for key of sedimentary log.

Fig. 11: Core photograph showing interval of marine incursion between 580.4 m and 579.35 m core depth. Note the subtle change from light grey to light red at inception of marine incursion.

Fig. 12: Total organic carbon weight (TOC) percentages of borehole 42/11 in correspondence to the $\delta^{13}C$ profile and the occurrence of inferred deep lake phases (dashed lines). Increased TOC during the negative excursion, the recovery stage, and during the subordinate phases of organic-rich deep lake sedimentation support a strong climatic control on lake sedimentology and bioproductivity.

Fig. 13: Depositional and ecological reconstruction of the Boltysh impact crater lake formation based on sedimentological and palynological data of borehole 42/11. The five lake stages recognised in the sedimentary log in Fig. 10 are here summarised to three major stages corresponding to the Early Danian carbon isotope profile. Plant data based on palynoflora examined in Jolley et al. (2010; 2013; 2015) and Daly & Jolley (2015). For details see text: fwwb – fair weather wave base.

Table 1: Sedimentological aspects of lithofacies identified in borehole 42/11.

Table 2: Facies associations of borehole 42/11 and their main characteristics. Lithofacies code based on numbers given in Table 1, with bolt numbers indicating the most indicative lithofacies in each facies association.

Table 3: Essential characteristics of lake stages based on analyses of borehole 42/11.

Lithofacies		Main features	Description
1	Clay-rich mud	Structureless, organic-rich	Structureless to faintly laminated (sub-mm scale), organic-rich, partially calcareous, medium grey to black, beds 20 to 40 cm thick
2	Clay-rich mud	Parallel laminated	Alternating couplets and triplets of clay, silt and organic matter (together <0.5 mm), partially calcareous, occasional calcite nodules, load structures, slickensides, synearesis cracks, plant remains, bioturbation, ostracods, fish remains, light grey to medium grey, individual beds 2 to 40 cm thick
3	Clay-rich mud	Parallel laminated, organic-rich	Laminated organic-rich mud and organic matter (together <0.5 mm), occasional silt laminae (<2 mm), microslumped and microfaulted, calcite nodules, plant remains, occasional ostracods, slickensides, medium grey to black, individual beds a few centimetres to 95 cm thick
4	Silt-rich mud	Parallel laminated	Laminated (typically <1 to 3 mm), often alternating with clay and organic-rich clay laminae, individual beds sometimes grading into clay and organic-rich clay, occasional stylolites, dewatering, clay-rich injection structures, ostracods, fish remains, plant remains, bioturbation, rootlets may be present, light to medium grey to brown-grey, individual beds 4 to 120 cm thick
5	Silt-rich mud	Wavy laminated	Lenticular to wavy laminated, occasionally faintly cross-laminated and climbing ripple laminated, (typically <1 to 3 mm), sets up to 1 cm, thin lenses of fine sand and clay-rich mud, small mud pebbles present, occasional synearesis cracks, low content of plant remains, ostracods and bioturbation, light brown to brown-grey, beds 2 to 150 cm thick
6	Silt-rich mud	Structureless	Structureless, often interbedded with parallel and wavy laminated mud, grading into laminated beds common, low content of plant remains and ostracods, light grey to grey brown and orange, individual beds a few centimetres to 15 cm thick
7	Marl	Parallel laminated or slumped	Carbonate-rich mud, faint discontinuous lamination present (5 to 12 mm), partially structureless or slumped, plant remains, light grey to light brown, individual beds up to 20 cm thick
8	Pebbly mud	Structureless with intra-formational clasts	Structureless to bedded (<5 cm), mudstone and marlstone intraclasts, quartz granules to pebbles, well rounded to subangular, plastic deformed in places, beds typically normal or reverse graded, slumping common, individual beds a few centimetres to 40 cm thick
9	Fine sand	Parallel laminated	Laminated arkosic sandstone (laminae 3 to 8 mm), good to moderate sorting, subrounded to subangular, low content of plant remains, light grey, occurs as isolated (partially lenticular) beds up to 23 cm thick
10	Fine to coarse sand	Structureless	Structureless, arkosic sandstone, poor to moderate, lenticular beds or continuous beds with sharp bases grading into laminated mud, occasional reverse grading, quartz and feldspar granules to small pebbles possible may be present, light to medium grey, individual beds up to 40 cm thick
11	Pebbly fine to coarse sand	Structureless with extra-formational clasts	Structureless, arkosic sandstone, poor to moderate sorting, subrounded to angular, subrounded to angular granules and small pebbles of quartz and feldspar, mudstone intraclasts, sandstones often grading into fine-grained sand and mud, occasional slumping, light to medium grey, individual beds 0.5 to 58.0 cm
12	Conglomerate	Structureless with extra-formational clasts	Structureless conglomerate of rounded to angular quartz and feldspar granules and pebbles, predominantly matrix-supported, often forms basis of graded beds, medium grey to brown grey, beds 5 to 22 cm thick
13	Calcite evaporites	Crystalline laminae	Crystalline calcium carbonate laminae (typically 1.0 to 1.5 mm, up to 5.0 mm), commonly no preferred orientation of crystals, occasional formation of stylolites, light to medium grey
14	Zeolite evaporites	Individual crystals mixed with siliciclastic sediment	Individual crystals (length <0.09 mm) of various zeolite phases (Heulandite-Clinoptilolite, Phillipsite), embedded in structureless and laminated clay-rich and silt-rich mud
15	Ostracod bioclast	Structureless to parallel laminated	Structureless to parallel laminated ostracod-rich marl and mud (laminae <1 to a few millimetres), occasional wavy lamination, normal grading common, beds of sharp boundaries, grading into siliciclastic mudstone common, plant debris and fish remains, light to medium grey, individual beds 5 to 30 cm thick
16	Carbonate micrite	Parallel laminated	Laminated carbonate micrite, (laminae <1 mm), light to medium grey, individual beds 3.5 to 11.0 cm thick

Facies association		Description	Interpretation	Lithofacies
FA_{MS}	Mud-rich shallow lake	Deposits of organic-rich and clay-rich mudstones and marlstones, structureless to faintly parallel laminated, interbedded with normal graded fine-grained sandstones and silt-rich mudstones, abundant rootlets, plant remains, ostracods, individual packages 20 to 40 cm thick	Deposition from suspension in vegetated, quiet, shallow water and swamp settings zones; may be subject to desiccation and early soil forming processes during phases of subaerial exposure	**1**, 2
FA_{SAS}	Sand-rich shallow lake	Wavy- and parallel laminated silt-rich mudstones and fine-grained sandstones (<3 mm), occasional oscillation ripples, abundant ostracods, fish remains, plant matter, occasional slumping and bioturbation, individual packages 20 to 400 cm thick	Transport via shore currents and increased wave activity, deposition above the fair weather wave base in shallow water, associated with increased river discharge and/or wind activity	2, 4, **5**, 7, **9**, 15, 16
FA_{SIS}	Silt-rich shallow lake	Parallel laminated silt-rich mudstones (<1 to 5 mm), interbedded with clay-rich and organic-rich mudstones, and thin lenticular layers of fine-grained sandstones; occasional occurrence of pebbly mudstone, micrite, marlstone and calcite and zeolite; bioturbation, plant matter, fish fossils and ostracods, individual packages are 5 to 450 cm thick	Deposition from suspension settling, together with overflows, interflows and underflows below the fair weather wave base in mostly shallow to transitional deep water	2, **4**, 6, 13, 14
FA_{DL}	Deep lake laminites	Parallel laminated clay, silt and organic matter forming couplets and triplets (together <1 mm); interbedded with thin layers of siltstone, sandstone, pebbly mudstone and crystalline calcite, slumping common, abundant bioturbation, fish fossils, plant matter, ostracods, individual packages are a few centimetres to 180 cm thick	Deposition through predominantly suspension settling in a deep lake setting, associated with occasional fine-grained turbidity currents and underflows, couplets and triplets represent seasonal changes in sediment and organic matter supply	**2**, **3**, **4**, 6, 7, 13, 14
FA_{OD}	Organic-rich deep lake	Parallel laminated organic-rich mudstone together with couplets of organic matter and clay (<1 mm), may be interbedded with thin layers of crystalline calcite and pebbly mudstone, abundant micro-slumping, small calcite nodules common, occasionally ostracods, individual packages are a few centimetres to 120 cm thick	Deposition from suspension settling, under mostly anaerobic conditions in a deep lake setting, low sediment supply, alternating with occasional clastic input through turbidity currents	2, **3**, 13, 14
FA_{CT}	Coarse-grained turbidites	Structureless (pebbly) fine to coarse-grained sandstones and conglomerates, typically grading into parallel-laminated silt-rich or clay-rich mudstones; associated with slumping features, sharp bases, erosive in places, occasional plant matter and mud-rip up clasts, individual packages are 2 to 290 cm thick	Transport and deposition through relative proximal turbidity currents, associated with phases of crater flank collapse and increased river discharge	4, 8, 9, **10**, **11**, **12**
FA_{FT}	Fine-grained turbidites	Wavy- and parallel laminated silt-rich mudstones (<1 to 3 mm) and graded structureless fine-grained sandstones, occasionally cross-laminated, partially grading into thick packages of laminated mudstone, comprises ostracod bioclasts, marlstone and micrites; sometimes associated with small-scale slumping, abundant plant remains, individual packages are a few millimetres to 32 cm thick	Transport and deposition through relative distal turbidity currents, associated slope failure, river discharge and with coarse-grained turbidites from more proximal settings	**4**, 6, 7, **9**, **10**, 15, 16
FA_{D}	Debris-flow deposits	Structureless, pebbly mudstones, conglomerates and (pebbly) sandstones, partially muddy matrix, non-graded, sometimes reverse graded, sedimentary clasts occasionally plastically deformed, sharp boundaries, individual beds are up to 80 cm thick	Transport and deposition through cohesive debris flows to non-cohesive sand-dominated hyperconcentrated density flows, associated with slope failure and crater flank collapse; may turn into turbidity currents	**8**, 10, **11**, **12**

Lake stage	Climate	Major facies	Lake type	Hydrology	Water chemistry
1 (pre-excursion)	Fluctuating warm temperate and winterwet	FA_{FT}, FA_{CT}, F_{D}, FA_{SIS}	Shallow, non-stratified, meromictic	Surface runoff, precipitation, groundwater	Fresh water
2 (negative excursion)	Dry winterwet	FA_{OD}, FA_{DL}, FA_{SIS}	Deep, stratified, meromictic to holomictic	Seasonal fluctuations, groundwater supply	Saline - alkaline
3 (mid-excursion)	Dry winterwet	FA_{DL}, FA_{SIS}, FA_{SAS}	Deep, stratified, meromictic to holomictic	Seasonal fluctuations, groundwater supply	Saline - alkaline
4 (recovery)	Cooling, temperate	FA_{SAS}, FA_{SIS}	Shallow, non-stratified, meromictic	Surface runoff, precipitation, groundwater	Brackish
5 (post-excursion)	Cooling, temperate	FA_{SAS}, FA_{SIS}	Shallow, non-stratified, meromictic	Surface runoff, precipitation	Fresh water

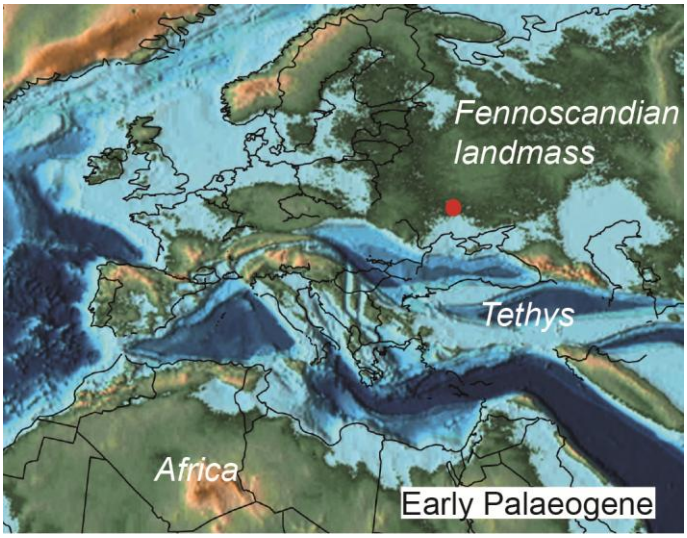

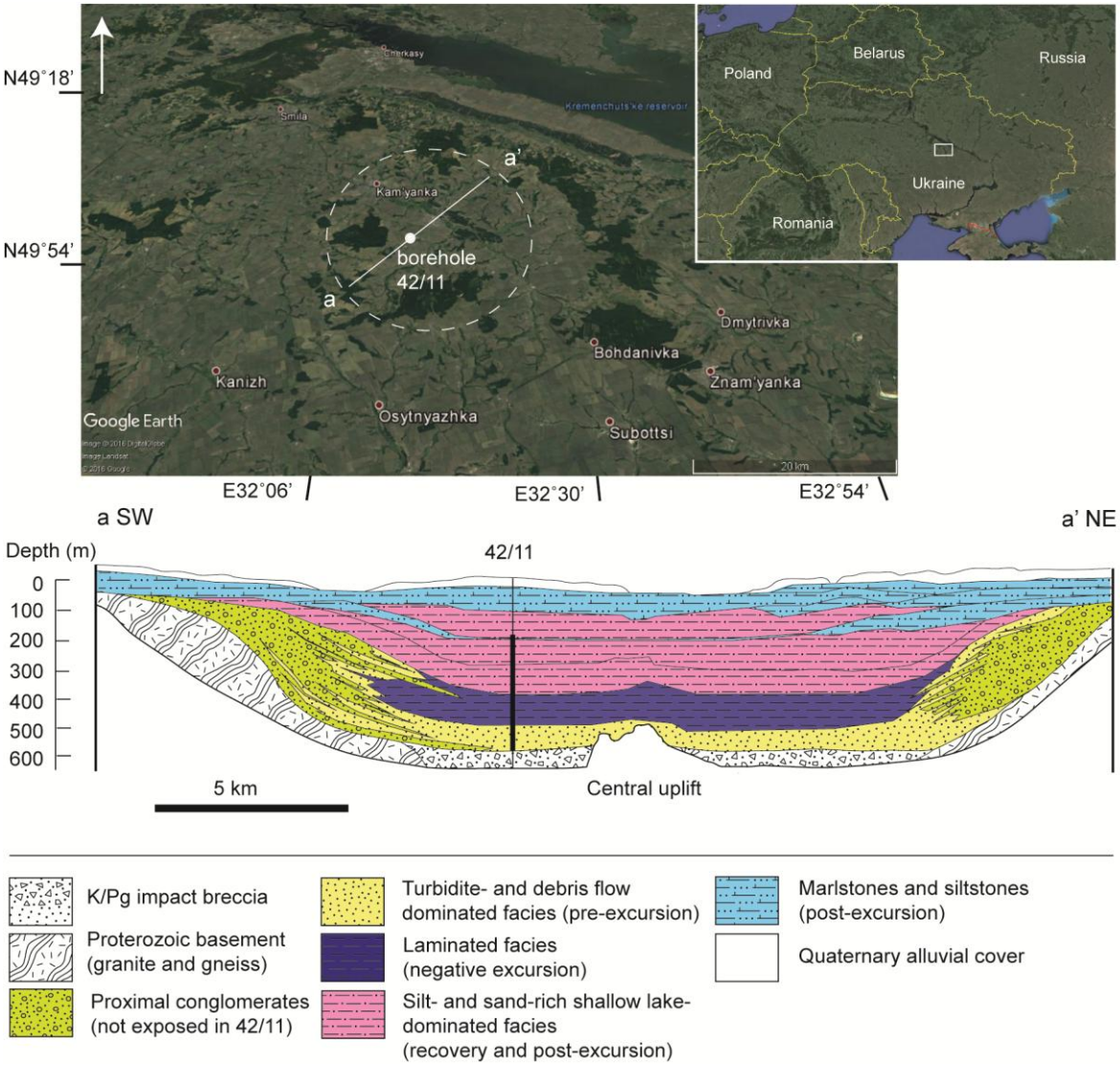

Lithofacies

- Impact breccia
- Clay-rich mudstone, parallel laminated
- Organic-rich mudstone, parallel laminated
- Interlaminae of silt- and clay-rich mudstone
- Silt-rich mudstone, parallel laminated or structureless
- Silt-rich mudstone, wavy laminated
- Fine- to medium-grained sandstone, structureless
- Fine-grained sandstone, parallel bedded
- Conglomerate, structureless
- +++ Calcite evaporites

Facies associations

- FA_{MS}: Mud-rich shallow lake
- FA_{SAS}: Sand-rich shallow lake
- FA_{SIS}: Silt-rich shallow lake
- FA_{DL}: Deep lake laminites
- FA_{OD}: Organic-rich deep lake
- FA_{D}: Debris flow deposits
- $FA_{FT/CT}$: Fine-/coarse-grained turbidites

Sedimentary structures and fossils

- Water escape
- # Slickensides
- Stylolites
- Synaeresis cracks
- Rip-up clasts
- Calcite nodules
- Carbonaceous debris
- Fish skeletons
- Rootlets
- Bioturbation
- Leaves
- Ostracods
- Gastropods